Petrogenesis of the Paleoproterozoic Näränkävaara layered intrusion, northern Finland, Part II: U-Pb ID-TIMS age and Sm–Nd isotope systematics

VILLE JÄRVINEN[1]*, TAPIO HALKOAHO[2], JUKKA KONNUNAHO[3], JUSSI S. HEINONEN[1], SANDRA KAMO[4], SARAH DAVEY[5], WOUTER BLEEKER[5], TUOMO KARINEN[3] AND O. TAPANI RÄMÖ[1]

[1]*Department of Geosciences and Geography, P.O. Box 64, FIN-00014 University of Helsinki, Finland*

[2]*Geological Survey of Finland, P.O. Box 1237, FIN-70211 Kuopio, Finland*

[3]*Geological Survey of Finland, P.O. Box 77, FIN-96101 Rovaniemi, Finland*

[4]*Department of Earth Sciences, University of Toronto, 22 Ursula Franklin Street, Toronto, M5N 1J8, Canada*

[5]*Geological Survey of Canada, 601 Booth Street, Ottawa, K1A 0E8, Canada*

Abstract

Several mafic-ultramafic layered intrusions were emplaced in the NE Fennoscandian Shield during a magmatic episode at 2.44 Ga. The Paleoproterozoic Näränkävaara layered intrusion, northern Finland, is one of the largest ultramafic bodies in the Fennoscandian Shield, with a surface area of 25 km x 5 km and a magmatic stratigraphic thickness of ~3 km. The intrusion comprises a 1.3 km-thick peridotitic–dioritic layered series (2436 ± 5 Ma) with two peridotitic reversals, and a 1.5–2 km thick basal dunite series mainly composed of olivine adcumulates (dated here). The intrusion has been studied since the 1960's, but several questions regarding its structure and petrogenesis remain. The basal dunite shows several lithological features typical of komatiitic rather than intrusive olivine cumulates; namely, >1 km-thick "extreme" olivine adcumulates, some showing textures with bimodal grain sizes, oscillating variations in Mg# with stratigraphic height, and poikilitic chromite. With Archean greenstone belts nearby, it was previously hypothesized that the basal dunite series could represent an Archean komatiitic wall rock to the Paleoproterozoic layered series. However, our new U-Pb ID-TIMS baddeleyite age of 2441.7 ± 0.9 Ma for the basal dunite series shows that the basal dunite and layered series of the Näränkävaara intrusion are co-genetic. New whole-rock Sm-Nd isotope data from key stratigraphic units (initial ε_{Nd} at 2440 Ma of -3.5 to -1.7) indicate that the intrusion was constructed from repeated emplacement of LREE-enriched high-MgO basaltic magmas that were mantle-derived and contaminated by crust, similarly to other Fennoscandian 2.44 Ga intrusions. The parental magmas show similar compositions regardless of stratigraphic position, suggesting that most wall rock contamination and homogenization had occurred before emplacement, with in situ contamination being a relatively minor process. The open-system features of the basal dunite suggest that it may have formed (at least partly) as a feeder channel cumulate, possibly related to the ~100 km long Koillismaa-Näränkävaara Layered Igneous Complex. The Näränkävaara parental magmas show variably depleted metal ratios and could have potential for orthomagmatic mineral deposits, given the availability of S-rich wall rocks.

*Corresponding author (e-mail: ville.jarvinen@helsinki.fi)

1. Introduction

Over 30 mafic-ultramafic layered intrusions are found in the NE Fennoscandian Shield, mainly in Finland and Russia (Fig. 1) (Alapieti et al. 1990). The intrusions are mostly located in discontinuous belts in the Kola and Karelian cratons with ages ranging between 2.53–2.40 Ga (Bayanova et al. 2019). Intrusions in the Karelian craton cluster in age around 2.44 Ga, with several of these hosting orthomagmatic ore deposits (Iljina & Hanski 2005; Iljina et al. 2015). Parental magma compositions of the Fennoscandian intrusions are relatively similar, with trace-element and isotope systematics suggesting a crustally contaminated mantle-plume related asthenospheric source (Huhma et al. 1990; Amelin et al. 1995; Puchtel 1997; Hanski et al. 2001a; Kulikov et al. 2010; Yang et al. 2016). Strong evidence linking the 2.44 Ga intrusions to komatiites in the Vetreny belt also support the mantle-plume hypothesis (Puchtel 1997; Hanski et al. 2001b). It has been suggested that these magmas could have been distributed over large distances by a deep crustal magma plumbing system (Hanski et al. 2001a).

The Koillismaa-Näränkävaara Layered Igneous Complex (KLIC), northern Finland (inset Fig. 1), comprises two mafic-ultramafic intrusions connected by a linear unexposed positive magnetic and gravity anomaly, with a total length of about 100 km (Alapieti 1982; Karinen 2010; Järvinen et al. 2020, 2021). It has been suggested that the 100 km long KLIC could represent a singular magmatic system (Alapieti 1982) and that it could be linked to a large-scale magmatic plumbing system connecting the Fennoscandian intrusions (Hanski et al. 2001a). Such large magmatic system could have significant potential for orthomagmatic mineral deposits (Begg et al. 2010; Maier & Groves 2011; Barnes et al. 2016; Begg et al. 2018; Lesher 2019).

The subject of this study is the large mafic-ultramafic Näränkävaara intrusion, the easternmost intrusion in the KLIC (Fig. 1). New data have become available since the previous major study in the area (Alapieti 1982), largely compiled and interpreted in previous studies (Järvinen et al. 2020, 2021, 2022). The Näränkävaara intrusion has a total stratigraphic height of ~3 km, divided about equally between two cumulate series (Fig. 2): 1) a 1.3 km-thick harzburgitic–dioritic layered series, dated at 2436 ± 5 Ma (Alapieti 1982), and 2) a 1.5–2 km-thick dunitic basal dunite series, undated before this paper. The main objective of this study is to examine the age and origin of the Näränkävaara basal dunite series, and to clarify its petrogenetic relationship to the layered series.

The basal dunite series exhibits several lithologic features that suggest high rate of magma flow-through and olivine accumulation with relatively low degree of ponding and differentiation (Järvinen et al. 2021), similar to what is typically described from high-volume channelized komatiite flows (Gole & Barnes 2020). Criteria in favor of this include an over 1 km-thick stratigraphic section composed of low-porosity ("extreme") olivine adcumulates (BD-2 in Fig. 2b), with most samples showing poikilitic chromite, so far only described from komatiitic systems (Godel et al. 2013), and few also showing textures with bimodal olivine grain-sizes. Oscillating variation in olivine adcumulate Fo contents with height is also observed (Arndt et al. 2008). As the nature of the contacts between the Näränkävaara basal dunite and layered series has remained unclear (Järvinen et al. 2020, 2021), and because there are two Archean greenstone belts neighboring the Näränkävaara intrusion (GB in Fig. 2) – both containing komatiitic olivine cumulates (Iljina 2003; Sorjonen-Ward & Luukkonen 2005; Makkonen et al. 2017; Karampelas 2022) – it was hypothesized that the Näränkävaara basal dunite could represent an Archean komatiitic wall rock to the Paleoproterozoic layered intrusion magmatism (Järvinen et al. 2021). Alternatively, based on similarities in major and trace element compositions between parental magma compositions inferred independently for the layered series and the basal dunite series, it was hypothesized that the basal dunite series was co-genetic with the layered series, and that the open-system features

Figure 1. Geological map of the central and northern Fennoscandian shield showing the distribution of 2.53–2.39 Ga mafic-ultramafic layered intrusions. Dotted line outlines the intrusions of the Tornio-Näränkävaara belt (TNB) in northern Finland. The Koillismaa-Näränkävaara Layered Intrusion Complex (KLIC; outlined in black) comprises the fragmented Koillismaa intrusion to the west, Näränkävaara intrusion to the east, and a connecting positive magnetic and gravity anomaly presumed to be a "hidden dyke" (Alapieti 1982). Inset shows KLIC on an aeromagnetic map (hill-shaded from the NE); Paleoproterozoic intrusions outlined in red and the "hidden dyke" outlined with red dash; Archean greenstone belts (GB) outlined in green. Map modified after Alapieti et al. (1990) and Karinen (2010).
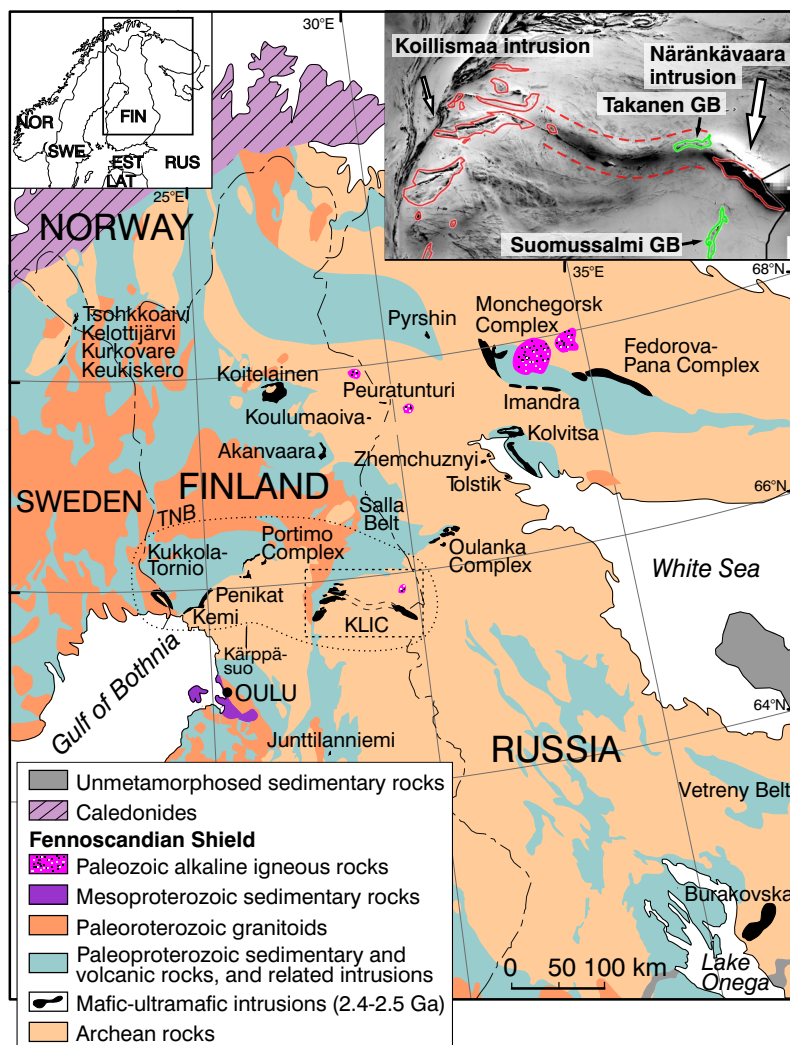
formed as feeder channel cumulates connected to the ~100 km long KLIC (Fig. 1) (Järvinen et al. 2021).

Our new U-Pb ID-TIMS baddeleyite age of 2441.7 ± 0.9 Ma for the basal dunite series confirms that it is co-genetic with the layered series. At least six lithological reversals have been inferred from the Näränkävaara intrusion, all attributed to magmatic recharge (Järvinen et al. 2020, 2021). Our new Sm-Nd isotopic data from key stratigraphic units throughout the intrusion (average initial ε_{Nd} of about -2 at 2440 Ma) indicate that it has formed by repeated intrusion of compositionally similar parental magmas, with similar LREE-enriched siliceous high-MgO basaltic (SHMB) compositions as found in other Fennoscandian 2.44 Ga intrusions (Kulikov et al. 2010; Huhma et al. 2018). We propose that the Näränkävaara basal dunite series represents, at least in part, an outcropping part of the KLIC feeder channel cumulate. Homogeneity of the Näränkävaara parental magma compositions, determined from several independent sources, suggests that large-scale crustal contamination preceded emplacement, and that contamination by in situ processes had a minor role only.

2. Geologic background

2.1. Koillismaa-Näränkävaara Layered Igneous Complex

The Näränkävaara intrusion is the easternmost of the Tornio-Näränkävaara belt of intrusions (TNB) (Fig. 1) (Alapieti et al. 1990). These 2.44 Ga intrusions were emplaced in an intracratonic rift setting and are presently located either within the Neoarchean granite-gneiss basement complex or between the basement complex and Paleoproterozoic rift-related volcanosedimentary cover sequences (Iljina & Hanski 2005). Two of the intrusive complexes (Penikat, Portimo) show evidence of repeated magmatic recharge in megacyclic stratigraphic units (Halkoaho 1993). These layered intrusions are economically important, hosting several orthomagmatic ore deposits (Iljina et al. 2015). Näränkävaara is exceptional in that about half of its cumulate stratigraphy is dominated by olivine adcumulates; the other intrusions are generally more pyroxenitic with minor peridotite and dunite. In this regard, Näränkävaara is similar to the dunite-rich Burakovsky intrusion in SE Karelia (Fig. 1) (Chistyakov & Sharkov 2008). Parental magmas of the Fennoscandian 2.44 Ga intrusions have been considered to be komatiitic or High-Mg basalts (average initial ε_{Nd} approximately –2, with 9–18 wt.% MgO and 0.5–1.0 wt.% TiO_2; Kulikov et al. 2010), sourced from a komatiitic primary magma contaminated with 5–20 % of Archean crust (Amelin & Semenov 1996; Hanski et al. 2001a; Yang et al. 2016).

The western intrusive members of the KLIC (Fig. 1) are, on average, more evolved (pyroxenitic–gabbroic) compared to the dunite–pyroxenite dominated Näränkävaara intrusion (Karinen 2010; Järvinen et al. 2020). A U-Pb age of 2436 ± 5 Ma (Alapieti 1982) was determined for the KLIC based on discordant multigrain TIMS analyses (Vaasjoki 1977) of zircon separates made from various rock types throughout the complex. Two of these dates were obtained from Gabbros of the Näränkävaara layered series, but the age

of the basal dunite series had, until the present study, remained unconstrained. The unexposed geophysical anomaly connecting the two intrusions (inset Fig. 1) was named the "hidden dyke" by Alapieti (1982) and speculated to represent a feeder channel to the KLIC. Recently, the Geological Survey of Finland conducted deep drilling over the anomaly and intersected ultramafic cumulates at a depth of 1400 m (Karinen et al. 2021). The anomaly overlaps with an Archean greenstone belt with S-bearing rock types (Takanen GB in Fig. 2a) and is a potential target for orthomagmatic mineral exploration.

2.2. Structure of the Näränkävaara intrusion

The mafic-ultramafic Näränkävaara intrusion (Fig. 2) is mostly unexposed and direct observations are primarily based on two discontinuous drilling profiles (*B* and *D* in Fig. 2c). Geophysical data indicate a surface footprint of about 25 km x 5 km, and that the intrusion extends to a depth of 5–10 km (Elo 1992). The intrusion is surrounded by steep contacts to the granite-gneiss basement complex, except at the NW tip where 50 m of volcanosedimentary rock is intersected at the southern-side contact (Vesanto 2003).

The intrusion comprises a total of five magmatic series, mostly composed of ultramafic cumulates. The magmatic stratigraphy of the main intrusive body is divided into two major cumulate series, which are the main topics of this study (Fig. 2b) (Järvinen et al. 2020, 2021):

1) a 1.5–2 km thick basal dunite series, mostly composed of homogeneous olivine adcumulates (dunite) with minor peridotite and pyroxenite;

2) a 1.3 km thick layered series, comprising a 700 m thick peridotitic-pyroxenitic ultramafic zone (UMZ), and a 600 m thick Gabbronoritic–dioritic mafic zone (MZ) – two peridotitic reversals are found, one in the UMZ and one in the MZ, both attributed to recharge by SHMB magma;

Figure 2. **a)** Simplified geological map of the Näränkävaara intrusion overlain on a hill-shaded digital elevation model. Stars labeled 1-6 indicate locations of new isotope samples (Table 3). The new U-Pb baddeleyite age is from sample number 2. Two Archean greenstone belts (GB) are labeled (Sorjonen-Ward & Luukkonen 2005; Karampelas 2022), and the geophysical "hidden dyke" anomaly outlined with dotted orange lines (Alapieti 1982). Inset: compilation of total magnetic intensity maps (warm = high). Intrusion outline in Russia compiled from online databases of the Russian Geological Research Institute (VSEGEI).

b) Approximate magmatic stratigraphic column of the Näränkävaara intrusion from combination of cross-sections *A* and *D*, with unit names and numbers presented for discussed units (MS = Marginal series, UMZ = ultramafic series, MZ = mafic series; basal dunite series unit numbers according to Järvinen et al. 2021).

c) Representative cross-sections *A–D* across the Näränkävaara intrusion.
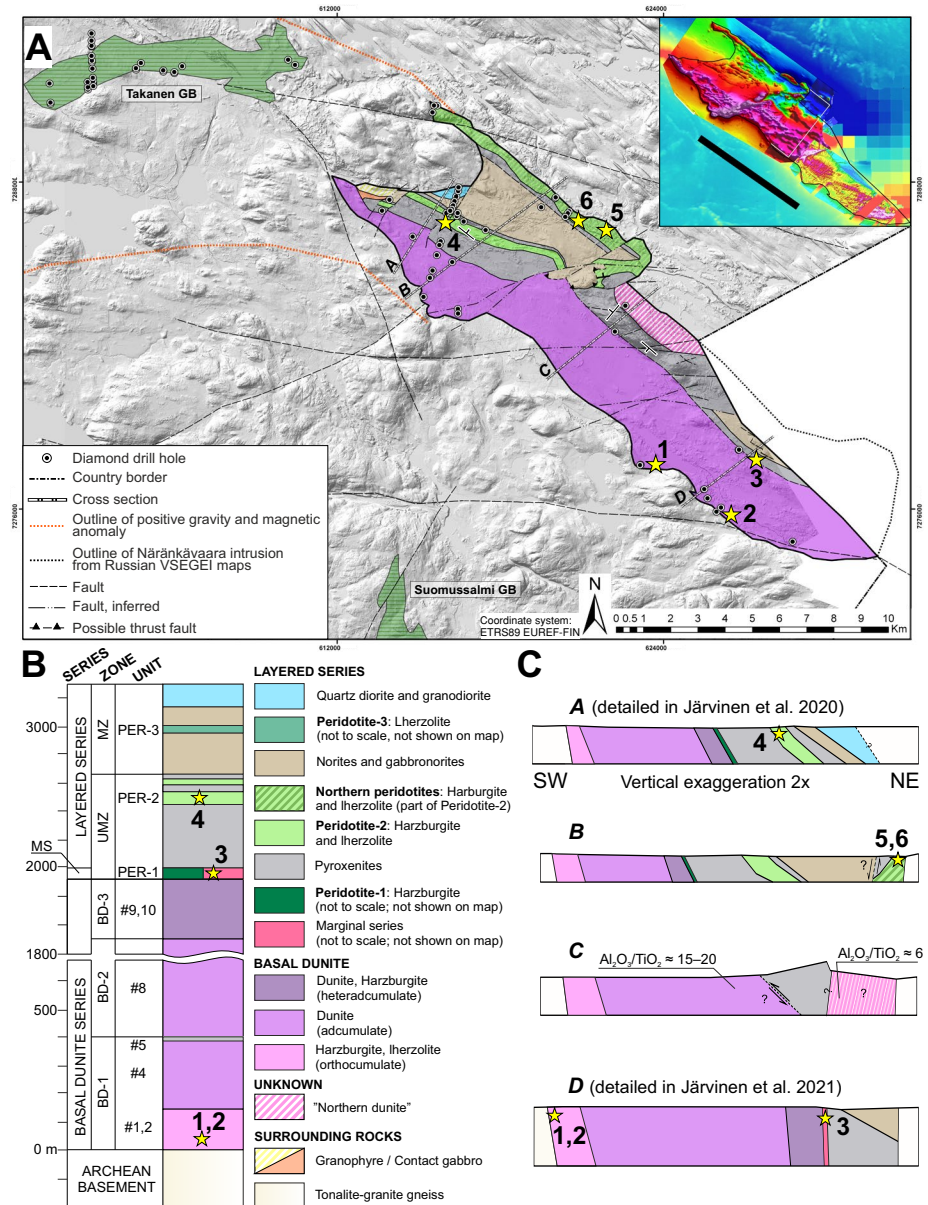
In addition, two smaller cumulate series are found at the margins of the intrusion (labeled in Fig. 2b):

3) a 200–400 m thick series of poikilitic harzburgites are found as "worm-like" elongate intrusions along the NW contact of the intrusion, called the "northern peridotites" – these have been correlated with the emplacement of the magma causing the first peridotitic reversal in the layered series (Järvinen et al. 2022);

4) a single drill hole along the NE contact of the intrusion intersects a "northern dunite" with significantly lower Al_2O_3/TiO_2 ratio compared to the basal dunite series (*C* in Fig. 2c); this unit is otherwise unknown and outside of the scope of this paper (see Akkerman 2008).

And, as final addition to the above:

5) a marginal series gabbronorite is found, as described below.

Table 1: Comparison of some petrological characteristics between key peridotitic units of the Näränkävaara intrusion

Series	Zone or Unit [1]	Lithology	(Mg+Fe)/Al (Si/Al)	(Mg/Al) (Fe/Al)	Forsterite mol. %	
					Calculated [2]	Analyzed [3]
Basal dunite Järvinen et al. (2020)	Zone BD-1 (high-Ni; unit #1)	Olivine orthocumulate (harzburgite–lherzolite)	1.85 (0.9975)	8.63 (0.9915)	89,6	88,6
	Zone BD-1 (moderate-Ni, unit #2)	Olivine orthocumulate (harzburgite–lherzolite)	1.99 (0.9963)	6.91 (0.9922)	87,4	88,0
	Zone BD-1 (moderate-Ni, unit #4)	Olivine adcumulate (dunite)	1.90 (0.9986)	6.55 (0.9935)	86,8	90.4[*]
	Zone BD-2 (low-Ni, unit #8)	Olivine adcumulate (dunite)	2.03 (0.9994)	6.95 (0.9848)	89,7	88.4[*]
	Zone BD-3 (low-Ni, units #9-10)	Olivine-orthopyroxene heteradcumulate & olivine-pyroxenite	2.01 (0.9938)	6.47 (0.9965)	86,6	87,6
Layered series Järvinen et al. (2021)	Unit PER-1 (basal peridotite in UMZ)	Olivine orthopyroxene adcumulate (harzburgite)	2.01 (0.9905)	6.35 (0.9908)	86,4	87,0
	Unit PER-2 (reversal in UMZ)	Olivine orthopyroxene mesocumulate (lherzolite)	1.83 (0.9386)	5.31 (0.9853)	84,2	84,3
	Unit PER-3 (reversal in MZ)	Lherzolite and olivine-pyroxenite	1.11 (0.4851)	3.49 (0.3543)	77,7	82,0
Northern peridotites Järvinen et al. (2022)	Unit OC	Olivine orthocumulate (harzburgite–lherzolite)	2.09 (0.9917)	6.97 (0.9977)	87,5	86,7
	Unit HAC	Olivine-orthopyroxene heteradcumulate (harzburgite)	2.01 (0.9909)	5.30 (0.9596)	84,1	85,9

Abbreviations: ultramafic zone (UMZ), mafic zone (MZ)

Element ratios calculated on a per-unit basis from all available whole-rock geochemical analysis[2] (in parentheses)

[1] For details on unit numbering and naming, see Fig. 5 in Järvinen et al. 2020 (layered series) and Table 1 in Järvinen et al. 2021 (basal dunite series)

[2] Calculated from Mg/Al vs. Fe/Al ratio according to method of Makkonen et al. (2017);

[3] Highest Fo analyzed with electron microprobe (Alapieti 1982; Telenvuo 2017; Järvinen et al. 2020, 2021);

[*] Highest whole-rock Mg# in serpentinized low-porosity olivine adcumulate

Cumulates generally become more evolved from the basal dunite (south) towards the top of the layered series (north), following the crystallization order Ol–Chr–Opx (basal dunite) and Ol–Chr–Opx–Cpx–Pl (layered series). The layered series is mostly unaltered, whereas the basal dunite is almost completely serpentinized. Both series are essentially undeformed with pristine or relict cumulus textures, except along fault planes.

A large SW-NE trending fault divides the intrusion into NW and SE blocks (Fig. 2a, note inset). The layered series shows well-developed modal layering in the UMZ and less-so in the MZ, with shallow but opposite dips in the NW and SE blocks. Visible (i.e., structurally measurable) igneous layering has not been observed in the basal dunite, but similar large-scale sequences of rock types and cryptic layering are found in both blocks (simplified cross-sections *B* and *D* in Fig. 2c). A contact between the two series has only been observed in drill core – in the NW block, rocks near the contact are strongly altered, but whole-rock geochemistry shows a small but distinct change to more evolved compositions towards the layered series. In the SW block, the contact is tectonic, with a non-cumulus textured marginal series gabbronorite formed on the side of the layered series (Fig. 2b and Table 1). The marginal series suggests

a hiatus in magmatism between the two series, however, its current location may also have been caused by post-magmatic faulting. It is possible that the SE-NW trending contact between the two series is tectonized along the entire length of the intrusion (Fig. 2a).

2.3. Peritotitic units of the Näränkävaara intrusion

Previous results suggest that the various peridotitic cumulates found in the Näränkävaara intrusion have been produced by repeated emplacement of high-MgO basaltic magmas (Alapieti 1982; Järvinen et al. 2020, 2021, 2022). The key petrological characteristics of the peridotitic units discussed in this section have been summarized in Table 1.

2.3.1. Basal dunite

Lithologically, the basal dunite series can be divided into three zones, labeled BD-1 to BD-3 in Fig. 2b (Järvinen et al. 2020, 2021). Zone BD-1 is relatively Ni-rich, and conversely zone BD-2 is relatively Cr-poor compared to the other two zones. The basal dunite series can be subdivided further into 10 units based on Mg#–Ni–Cr systematics (see labels in Fig. 2b) (Järvinen et al. 2021), but the simpler zone-based subdivision will mostly be used here, as described below:

BD-1 is about 300–500 m thick in total, and, from the basement complex contact upwards, is composed of (1) a 100–200 m thick olivine orthocumulate margin, grading upwards into (2) low-porosity "extreme" olivine adcumulates, and ending in (3) a thin unit of orthopyroxenite. The olivine orthocumulates are lherzolitic-harzburgitic in composition and in contact with the granite-gneiss basement to the south. Modal olivine increases rapidly (porosity decreases) with distance from the contact. The orthocumulates are characterized by few vol.% of phlogopite as well as clinopyroxene (Fig. 3). They show enrichment in incompatible elements (10–40 ppm Zr), and are inferred to be composed of linear mixes of cumulus olivine and trapped interstitial high-MgO basaltic melt. They are interpreted to have formed by rapid cooling against the basement rocks at the initial emplacement of the basal dunite series parental magma (Järvinen et al. 2021). Because of the trapped liquid component and enrichment in incompatible elements, this particular rock type was selected for detailed SEM imaging in pursuit of recoverable baddeleyite and zircon for geochronology.

BD-2 is about 1–1.3 km thick and entirely composed of low-porosity "extreme" olivine ad-cumulates (dunites) with <3 vol.% intercumulus (Järvinen et al. 2020, 2021). A ~1 km thick continuous interval of homogeneous adcumulate contains poikilitic chromite, typically described from channelized komatiite flows (Godel et al. 2013). Zone BD-2 can be characterized as untypically thick and homogeneous. Ultramafic basal zones are common in mafic intrusions (e.g. Burakovsky, Great Dyke, Munni Munni), but are typically composed of 10–100 m scale rhythmic sections of interlayered harzburgite and dunite, or contain layered chromitites (Wilson 1996; Hoatson & Keays 1989; Chistyakov & Sharkov 2008).

BD-3 is 200–500 m thick and marked by appearance of coarse-grained orthopyroxene oikocrysts. The zone is composed of olivine-ortho-pyroxene heteradcumulates (dunite-harzburgite) with interlayers of granular harzburgite. Geochemically, both BD-2 and BD-3 are very poor in incompatible elements.

Olivines in the basal dunite series range between Fo$_{85-91}$ (Table 1). Mg# generally decreases from south to north towards the layered series, but at least three reversals to more primitive compositions are found (Järvinen et al. 2021).

2.3.2. Layered series

The layered series includes a basal harzburgite (PER-1 in Fig. 2b and Table 1) and two peridotitic reversals: a more major lherzolitic one in the UMZ (PER-2) and a minor lherzolite/olivine-pyroxenite in the MZ (PER-3). Both reversals are distinct

olivine-rich units within more evolved cumulate sequences and have been interpreted to be caused by new magma pulses (Alapieti 1982; Järvinen et al. 2020). Average olivine Fo compositions decrease with each peridotitic unit (Table 1).

In Part I of this paper (Järvinen et al. 2022), we present evidence that the magma causing the PER-2 reversal in the layered series was emplaced along the NW contact of the intrusion. Emplacement of this magma formed a rapidly cooled olivine orthocumulate margin against the northern basement rocks, followed by olivine-orthopyroxene heteradcumulates towards the center of the intrusion to the south (units OC and HAC in Table 1, respectively); together, these are referred to as the "northern peridotites" (*B* in Fig. 2c). Lithologically, the northern orthocumulate margin (unit OC) is very similar to the stratigraphically much lower southern orthocumulate margin of the basal dunite series (unit BD-1 in Fig. 2b), except that it is slightly more evolved (see Table 1).

3. Isotope geochemical sampling and methods

3.1. Baddeleyite U-Pb ID-TIMS dating

The dated sample was obtained from drill hole R8 near the base of the basal dunite series, about 60 m above the contact with the Archean granite-gneiss basement (sample *2* in Fig. 2). The sample is an olivine orthocumulate with poikilitic pyroxenes and intercumulus phlogopite (Fig. 3), with relatively high concentrations of incompatible elements in whole-rock analysis indicating intercumulus melt (Järvinen et al. 2021). The sampled interval consisted of about 6 m (7.2 kg) of texturally homogeneous half-core with only minor fracturing. Scanning electron microscopy (SEM) of a single thin-section revealed about 20 baddeleyite crystals, 10–50 μm in size, typically fractured but otherwise well preserved and lacking secondary zircon overgrowths (Figs. 4b, c); apatite and rare

zirconolite were also identified. Mineral separation from a 5 kg sub-sample successfully recovered six baddeleyite grains, with two best preserved grains dated by U-Pb geochronological methods (see inset in Fig. 4a).

U-Pb analysis of the single baddeleyite grains was performed by isotope dilution–thermal ionization mass spectrometry methods (ID-TIMS) in the Jack Satterly Geochronology Laboratory at the University of Toronto. Baddeleyite was cleaned in 8N HNO_3 at room temperature prior to dissolution. A mixed ^{205}Pb-^{235}U spike was added to the Teflon dissolution capsules during sample loading. Single baddeleyite crystals were dissolved using 0.10 ml of concentrated HF and 0.02 ml of 8N HNO_3 at 200° C for 3 days. Samples were dried to a precipitate and re-dissolved in 0.15 ml of 3N HCl overnight (Krogh 1973). U and Pb were isolated from the baddeleyite solution utilizing miniaturized 50 μl anion exchange columns using HCl, dried in 0.05N H_3PO_4, deposited onto outgassed Re filaments with silica gel (Gerstenberger & Haase 1997), and analyzed with a VG354 mass spectrometer using a Daly detector in pulse counting mode. Corrections to the ^{206}Pb-^{238}U ages for initial ^{230}Th disequilibrium in the baddeleyite have been made assuming a Th/U ratio of 4.2 in the magma. All common Pb (0.1–0.2 picograms) was assigned to procedural Pb blank. Dead time of the measuring system for Pb and U was 16 and 14 ns, respectively. The mass discrimination correction for the Daly detector is constant at 0.05% per atomic mass unit. Amplifier gains and Daly characteristics were monitored using the SRM 982 Pb standard. Thermal mass discrimination corrections are 0.10 % per atomic mass unit for both Pb and U. Decay constants are those of Jaffey et al. (1971). A uranium isotopic composition of 137.88 was used (Steiger & Jager 1977). All age errors and error ellipses in the concordia diagrams are 2σ. VG Sector software was used for data acquisition. In-house data reduction software was used. Plotting and age calculations were done using Isoplot 3.31 (Ludwig 2003).
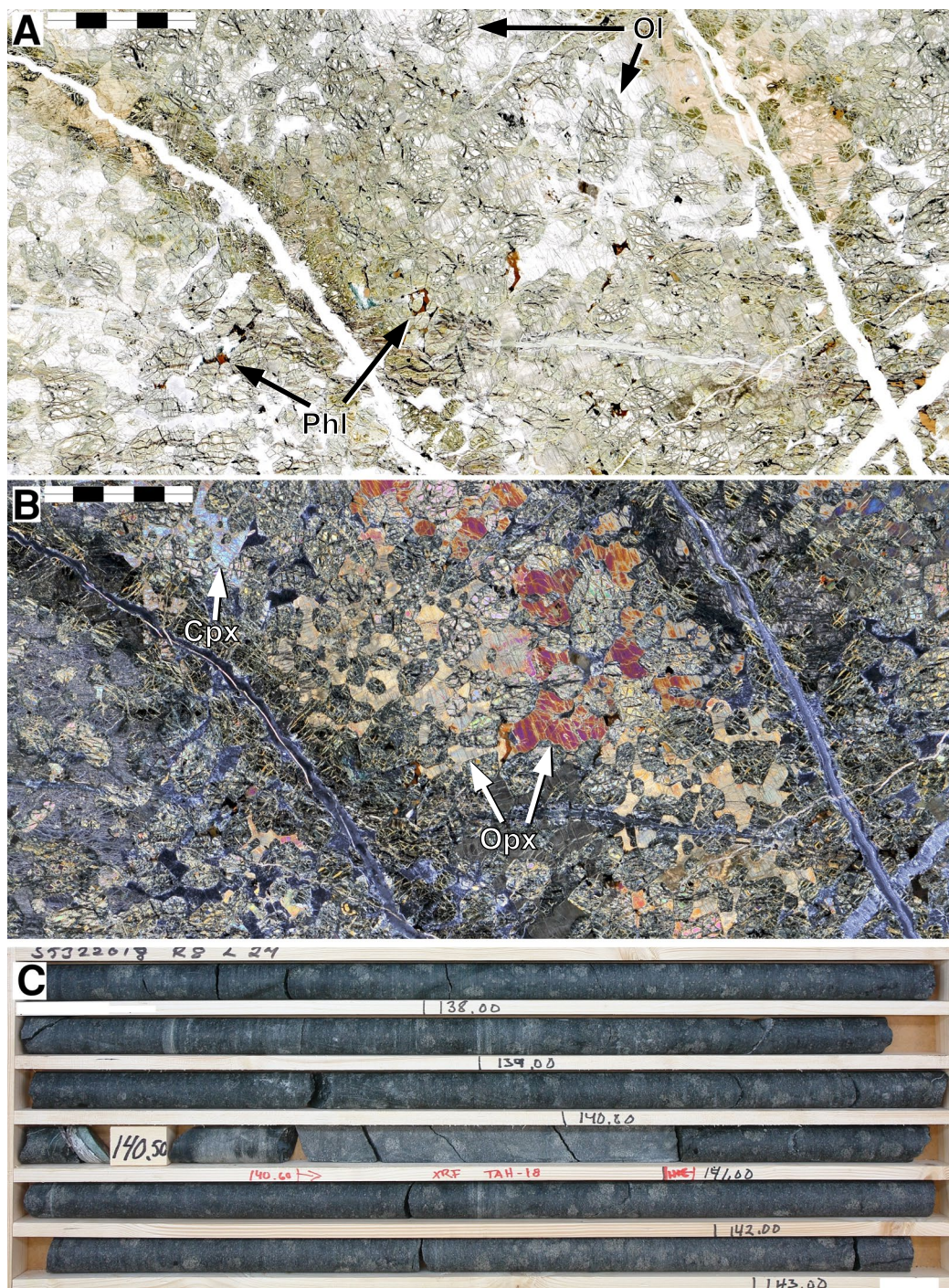
Figure 3. **a)** Plane-polarized and **b)** cross-polarized photomicrographs of olivine orthocumulate sample found at the southern basement complex contact of the basal dunite series of the Näränkävaara intrusion (BD-1 in Fig. 2b). Rock is mainly composed of serpentinized cumulus olivine with intercumulus of ortho- and clinopyroxene (poikilitic) and minor plagioclase and phlogopite. Scale bar is 5 mm; abbreviations are olivine (Ol), orthopyroxene (Opx), clinopyroxene (Cpx), phlogopite (Phl). **c)** Drill-core from hole R8 showing interval of homogeneous olivine orthocumulate (photos in **a** and **b** from R8 141.0 m, note red marker); split core from interval in photo was separated for baddeleyite (sample *2* in Fig. 2).

3.2. Whole-rock Sm-Nd

Six new whole-rock Sm-Nd isotope analyses were made from key stratigraphic units of the Näränkävaara intrusion (numbered *1–6* in Fig. 2): two samples (*1*, *2*) are from the olivine ortho-cumulate contact zone of the basal dunite; one (*3*) is from the marginal series gabbronorite; one (*4*) is from the first peridotitic reversal in the middle of the layered series (unit PER-2); and two (*5*, *6*) are from the northern peridotites.

Analyses were performed at the University of Austin, Texas. Powdered whole-rock samples (50–100 mg) were spiked and dissolved in a mixture of 29M HF and 14M HNO_3 in Teflon beakers in a 150 °C oven for 5 days, dried to salt, and, after adding 6M HCl, put back into the oven for 24 hours. Dried samples were re-dissolved in 15N HNO_3 to eliminate chlorides, followed by drying and dissolution in 2N HNO_3. The bulk REEs were isolated in 200 µl columns using BioRad AG50-X8 resin, the resulting fraction dissolved in 6N HCl and dried, re-dissolved in 0.3N HCl

and Nd isolated using prefilled calibrated columns filled with LN-SPEC resin. Samples were loaded on Re filaments in dilute H_3PO_4 and analyzed on double filaments with a Thermo Scientific Triton TIMS instrument. Signals of 1–4 V ^{144}Nd were measured for >80 ratios with 8 second integrations to generate 2σ absolute standard error of $6 \cdot 10^{-6}$ or better (typical ion intensities for ^{144}Nd were ~$2 \cdot 10^{-11}$ volts). Total procedural blanks of 7 pg Nd and 9 pg Sm were insignificant compared to amounts processed. Repeated analysis of a JNdi-1 standard (accepted 2σ-value of 0.512115 ± 0.000007) shows a long-term average of $^{143}Nd/^{144}Nd$ = 0.512114 ± 0.000013, which is within acceptable limits (external 2σ error equal to initial ε_{Nd} of ± 0.47 at 2440 Ma). The Nd isotopic ratios were corrected for fractionation using $^{146}Nd/^{144}Nd$ of 0.7219 and an exponential fractionation law. All ε_{Nd}-values were calculated using $\lambda^{147}Sm = 6.54 \cdot 10^{-12}$ and present CHUR values of $^{147}Sm/^{144}Nd$ = 0.1966 and $^{143}Nd/^{144}Nd$ = 0.512638.
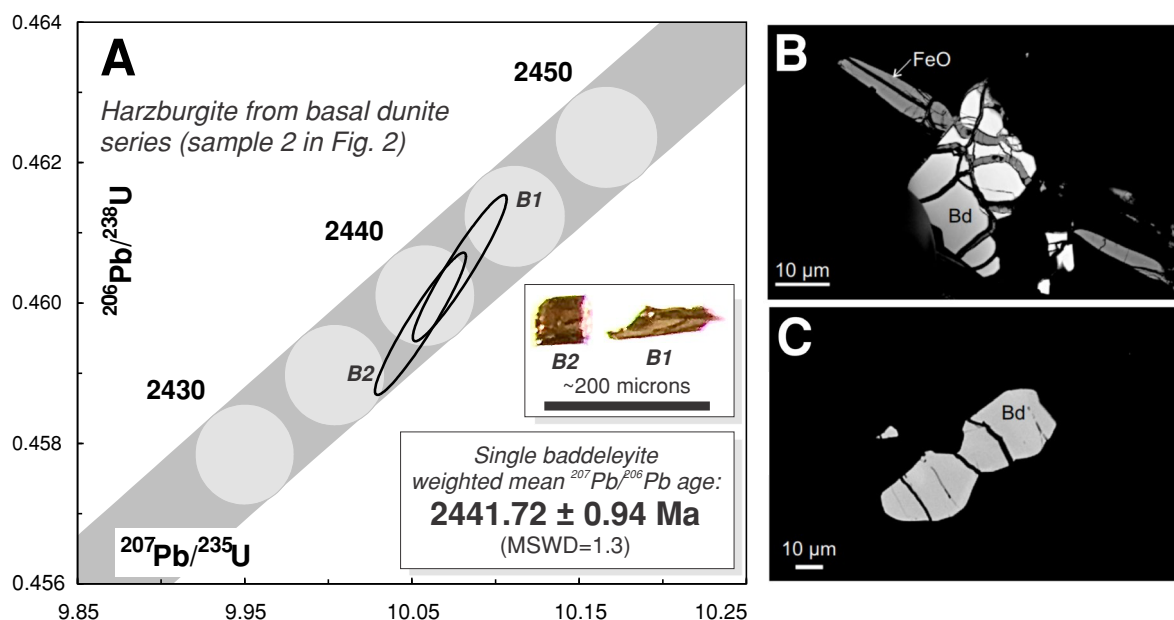

Fig. 4 a) Concordia diagram showing U-Pb ID-TIMS results for two baddeleyite grains from the basal dunite series of the Näränkävaara intrusion. Inset shows optical images of the baddeleyite grains analyzed in this study. Sample location where mineral separates were obtained is labeled *2* in Fig. 2 (drill hole R8, 137.50-143.15 m). **b)** and **c)** SEM back-scattered electron images of representative baddeleyite crystals (Bd) observed in thin section R8 141.00 m.
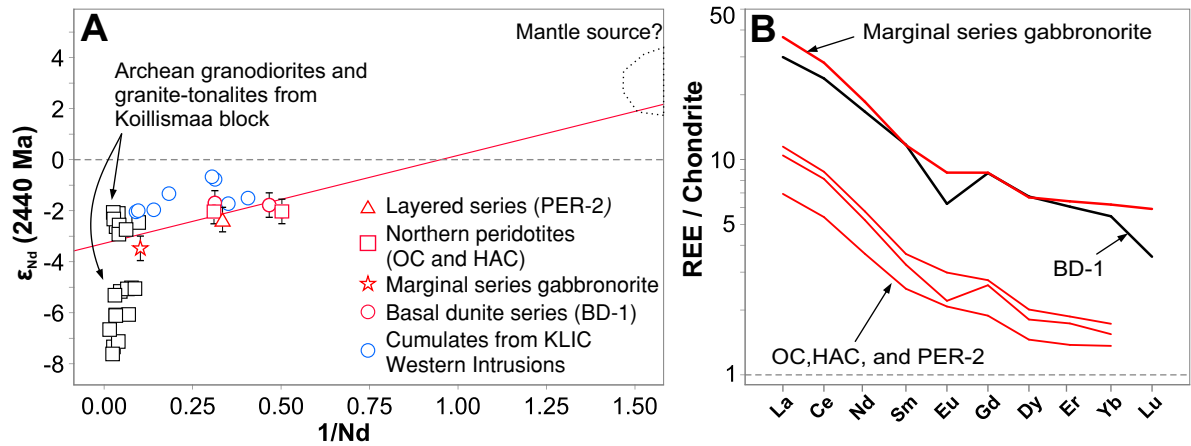
Figure 5. **a)** Sm-Nd isotope compositions of the Näränkävaara intrusion as demonstrated by results from six new whole-rock samples (red) on an initial ε$_{Nd}$(2440 Ma) vs. 1/Nd diagram (error bars show external 2σ-error of ± 0.5). Trend-line is interpreted as a mixing line between a Paleoproterozoic mantle-sourced magma and a crustal granitoid contaminant. Comparison to mafic cumulates from the Koillismaa intrusion of the Koillismaa-Näränkävaara Layered Igneous Complex (KLIC) are shown in blue. See Fig. 2 and Table 1 for abbreviated unit names. KLIC data from Karinen (2010); granitoid data from Hölttä et al. (2012). **b)** Chondrite-normalized REE-patterns of the new Sm-Nd samples (BD-1 based on model results from units #1 and 2 from Järvinen et al. 2021; others from this study).

Table 2: U-Pb ID-TIMS isotopic data for single-crystal baddeleyite fractions from harzburgitic olivine orthocumulate of the basal dunite series of the Näränkävaara intrusion

Analysis No.	Weight (µg)	U (ppm)	Th/U	Pb$_C$ (pg)	^{206}Pb/^{204}Pb measured	^{207}Pb/^{235}U	2s	^{206}Pb/^{238}U	2s	Error Corr	^{207}Pb/^{206}Pb	2s	^{206}Pb/^{238}U	2s	^{207}Pb/^{235}U	2s	^{207}Pb/^{206}Pb	2s	Disc %
															Age (Ma)				
B1	~2	168	0,02	0,1	87484	10,079	0,023	0,46049	0,00085	0,946	0,15874	0,00013	2441,72	3,75	2442,01	2,09	2442,26	1,33	0,03
B2	~2	270	0,01	0,2	72717	10,055	0,022	0,45969	0,00083	0,947	0,15864	0,00012	2438,19	3,66	2439,82	2,06	2441,18	1,32	0,15

Notes:

B is baddeleyite.

Th/U calculated from radiogenic ^{208}Pb/^{206}Pb ratio and ^{207}Pb/^{206}Pb age assuming concordance.

Pb$_C$ is total common Pb assuming the isotopic composition of laboratory blank:

assigned the isotopic composition of laboratory blank (206Pb/204Pb=18.49±0.4%; 207Pb/204Pb=15.59±0.4%;208Pb/204Pb=39.36±0.4%).

^{206}Pb/^{204}Pb corrected for fractionation and common Pb in the spike.

Pb/U ratios corrected for fractionation, common Pb in the spike, and blank.

Correction for ^{230}Th disequilibrium in ^{206}Pb/^{238}U and ^{207}Pb/^{206}Pb assuming Th/U of 4.2 in the magma.

Disc is percent discordance for the given ^{207}Pb/^{206}Pb age

Error Corr is correlation coefficients of X-Y errors on the concordia plot.

Decay constants are those of Jaffey et al. (1971) ^{238}U and ^{235}U are 1.55125 X 10^{-10}/yr and 9.8485 X 10^{-10}/yr.

^{238}U/^{235}U ratio of 137.88 used for ^{207}Pb/^{206}Pb model age calculations.

Table 3: Sm-Nd ID-TIMS whole-rock isotope data from the Näränkävaara intrusion (sample locations marked in Fig. 2

Sample #	Series	Unit [a]	Sm ppm	Nd ppm	^{147}Sm/^{144}Nd ± 0.00007	^{143}Nd/^{144}Nd	Initial ^{143}Nd/^{144}Nd (2440 Ma)	ε$_{Nd}$ (2440 Ma) ± 0.5
1	basal dunite	#1	0,46	2,14	0,1295	0.511468 ± 9	0,509385	-1,8
2	basal dunite	#2	0,66	3,20	0,1255	0.511408 ± 5	0,509389	-1,7
3	marginal series		1,98	9,77	0,1227	0.511271 ± 7	0,509298	-3,5
4	layered series	PER-2	0,61	2,99	0,1226	0.511328 ± 11	0,509356	-2,4
5	layered series	HAC	0,42	1,99	0,1274	0.511421 ± 8	0,509372	-2,0
6	layered series	OC	0,66	3,22	0,1231	0.511352 ± 6	0,509372	-2,0

[a] For details on unit numbering and naming, see Fig. 5 in Järvinen et al. 2020 (layered series) and Table 1 in Järvinen et al. 2021 (basal dunite series).

Sample numbers: *1*) R6 89.70; *2*) R8 140.60; *3*) R1 173.65; *4*) VJJA-48 (outcrop) ; *5*) VJJA-51 (outcrop) ; *6*) VJJA-76 (outcrop).

Errors (2σ) in isotope ratios based on within-run statistics of repeated standard measurements.

4. Results of U-Pb and Sm-Nd isotope analyses

The two analyzed baddeleyite grains from the basal dunite series produced concordant results with overlapping $^{207}Pb/^{206}Pb$ dates that give a weighted mean age of 2441.7 ± 0.9 Ma (Table 2 and Fig. 4). U-Pb dates show slightly higher errors compared to Pb-Pb results (Table 2), but all indicated age ranges (2438–2442 Ma) are within error and compatible with the old multigrain zircon U-Pb age of the KLIC and the Näränkävaara layered series (2436 ± 5 Ma; Alapieti 1982).

Results of six new whole-rock Sm-Nd isotope analyses are presented in Table 3 and Fig. 5. Variance in sample $^{147}Sm/^{144}Nd$ ratios is too small to permit calculation of a Sm-Nd isochron age. Four of the samples are olivine cumulates with Nd ranging between 2.0–3.2 ppm, and one gabbronorite sample containing 9.7 ppm Nd. Initial ε_{Nd}-values calculated at 2440 Ma (external 2σ error of ± 0.5) range between -1.8 and -2.4, and while ε_{Nd} appears to decrease upwards in stratigraphy from the basal dunite to the layered series, the differences between units are not statistically significant (Table 3). Exception is the marginal series gabbronorite which shows the most unradiogenic initial ε_{Nd} (-3.5), suggesting a slightly larger input of Archean crustal material (Fig. 5a).

5. Discussion

5.1. Co-genetic origin of the Näränkävaara basal dunite and layered series

The dated baddeleyite separate was obtained from the southern olivine orthocumulate margin of the basal dunite series (sample *2* in Fig. 2). This orthocumulate unit was formed by rapid cooling against the basement gneiss (Järvinen et al. 2021). Baddeleyite is highly refractory, and in layered intrusions is thought to have formed from primary magma and record the age of magmatic

crystallization (Bayanova 2006). We interpret the new baddeleyite age of 2441.7 ± 0.9 Ma as the time of crystallization of the orthocumulate unit (Fig. 4). This disproves the "Archean komatiitic wall rock" hypothesis discussed previously (Järvinen et al. 2021) and indicates that the basal dunite series is co-genetic with the 2436 ± 5 Ma layered series (Alapieti 1982). The most primitive parental magma composition for the Näränkävaara intrusion has been inferred from the trapped liquid component in this newly dated olivine orthocumulate unit (13–18 wt.% MgO, Fo_{89-90}, and 700 ppm Ni; see unit #1 in Table 1) (Järvinen et al. 2021) and thus this new baddeleyite age most likely marks the beginning of the emplacement of the Näränkävaara intrusion. This age is similar to that obtained for other 2.44 Ga mafic intrusions in Finland and Russia (Fig. 1), with the most similar zircon U-Pb ages obtained from the Kärppäsuo (2444 ± 4 Ma) dyke-like body and the small Junttilanniemi (2443 ± 7 Ma) intrusion (Konnunaho & Lahti 2008; Halkoaho & Niskanen 2011; Huhma et al. 2018).

A co-genetic origin for the basal and layered series is also supported by the new Sm-Nd isotope results (Table 3 and Fig. 5) with similar initial ε_{Nd} values of about -2 throughout the magmatic stratigraphy of the intrusion (sample numbers *1-6* in Fig. 2). These are similar to the initial ε_{Nd} values of the western KLIC intrusion blocks (Fig. 5) (Karinen 2010; Rämö et al. 2017; Huhma et al. 2018) and other 2.5–2.4 Ga intrusions in Fennoscandia (Kulikov et al. 2010).

5.2. Formation of the basal dunite series in open magma system

Recently, ultramafic cumulates were discovered along the "hidden dyke" geophysical anomaly that connects the intrusions of the KLIC (Karinen et al. 2021) and it seems plausible that the KLIC forms a continuous ~100 km long magmatic system, as previously suggested by Alapieti (1982) and Hanski et al. (2001a). Several "komatiite channel-like" open-system lithologic features are found in the

Näränkävaara basal dunite series. We suggest that the basal dunite series could have formed, at least partly, in an open magma channel environment. Four criteria favor open-system evolution of the Näränkävaara basal dunite:

1) *The high proportion of "extreme" low-porosity olivine adcumulates, with a maximum uninterrupted sequence over 1 km thick* (BD-2 in Fig. 2b). This raises the question of mass balance in a scenario of a single magma batch. Fractional crystallization modeling (using the Magma Chamber Simulator running the MELTS engine version 1.2.0.; Gualda et al. 2012; Bohrson et al. 2020) of inferred Näränkävaara parental magmas with up to 18 wt.% MgO (Järvinen et al. 2020, 2021) and at 0.5–2 kbar and Fe^{3+}/Fe_{tot} of 0–0.1 results in a maximum of about 20 % olivine. This indicates a minimum height of ~5 km for magma column needed to produce the basal dunite series from a single batch of magma. Similarly, the weighted average composition of cross-section *A* in Fig. 2c is 33 wt.% MgO if the basal dunite series is included (Järvinen et al. 2020), which is incompatible with the inferred maximum Fo_{90-91} (Table 1), but only 15.6 wt.% MgO if the basal dunite series is excluded (cf. 14.5 wt.% in the marginal series). These calculations strongly suggest that the olivine adcumulates in the basal dunite series have formed by incremental accumulation of olivine in an open magmatic system

2) *Oscillating back-and-forth fluctuations in olivine adcumulate Mg# along drill core intersections* ($Fo_{87.5-90.4}$ in unit #4 in Table 1) (Järvinen et al. 2021). Simplest explanation for this is variance in overlying, or overflowing, magma composition from which olivine is crystallizing, as commonly described from komatiite flows (Hill et al. 1995; Arndt et al. 2008).

3) *Bimodal olivine grain size distribution is found in some of the olivine adcumulate thin-section samples.* This may form by thermo-mechanical erosion and transport of previously formed cumulates, or mechanical sedimentation of suspended phenocrysts (Arndt et al. 2008). Note that our data is based on visual estimation from a limited number of thin-sections, and the amount and distribution of these bimodal adcumulate samples in the basal dunite is poorly constrained.

4) *A ~1 km thick sequence of olivine adcumulates with coarse (<2 mm) poikilitic chromite in zone BD-2* (unit #8 in Fig. 2b) (Järvinen et al. 2021). Poikilitic chromite is common in high-temperature ($>Fo_{92-93}$) komatiitic cumulates (Barnes 1998). While euhedral and intercumulus chromites are common in mafic-ultramafic intrusions (e.g., Wilson 1996), true coarse-grained poikilitic chromite has not been described from such settings except in the Näränkävaara basal dunite (and possibly the Dumont "komatiitic sill" in Canada; see Duke 1986). Thermo-chemical factors, mainly high temperature and low oxygen fugacity, can inhibit chromite nucleation so that once nucleation occurs it leads to fast growth of poikilitic chromite from Cr-supersaturated magma (Barnes 1998; Godel et al. 2013; Latypov et al. 2020). Because of relatively low olivine Fo content ($<Fo_{91}$), it is unlikely that the occurrence of poikilitic chromite in the Näränkävaara basal dunite series is related to high temperatures, but rather to low oxygen fugacity of the parental magma as inferred from the low poikilitic chromite Fe^{3+}# values (0.02–0.10) (Murck & Campbell 1986; Järvinen et al. 2021). Järvinen & Halkoaho (2022) suggested that the initially emplaced marginal olivine orthocumulates (with more oxidized chromites) insulated later magma pulses from oxidizing interactions with wall rocks, thus retaining their original relatively reduced magma compositions and resulting in growth of poikilitic chromite. Barnes (1998) also noted that poikilitic chromite is typically found in below-cotectic proportions in channel-facies komatiitic cumulates, and that some kinematic-mechanical processes, for example fast flowing magma, flushes the Cr-enriched residual melt and any small chromite nuclei downstream. The Näränkävaara poikilitic chromite is also found in below-cotectic proportions, possibly indicating high magma flow rates.

Olivine adcumulates are described from both mafic-ultramafic intrusions and komatiite flows,
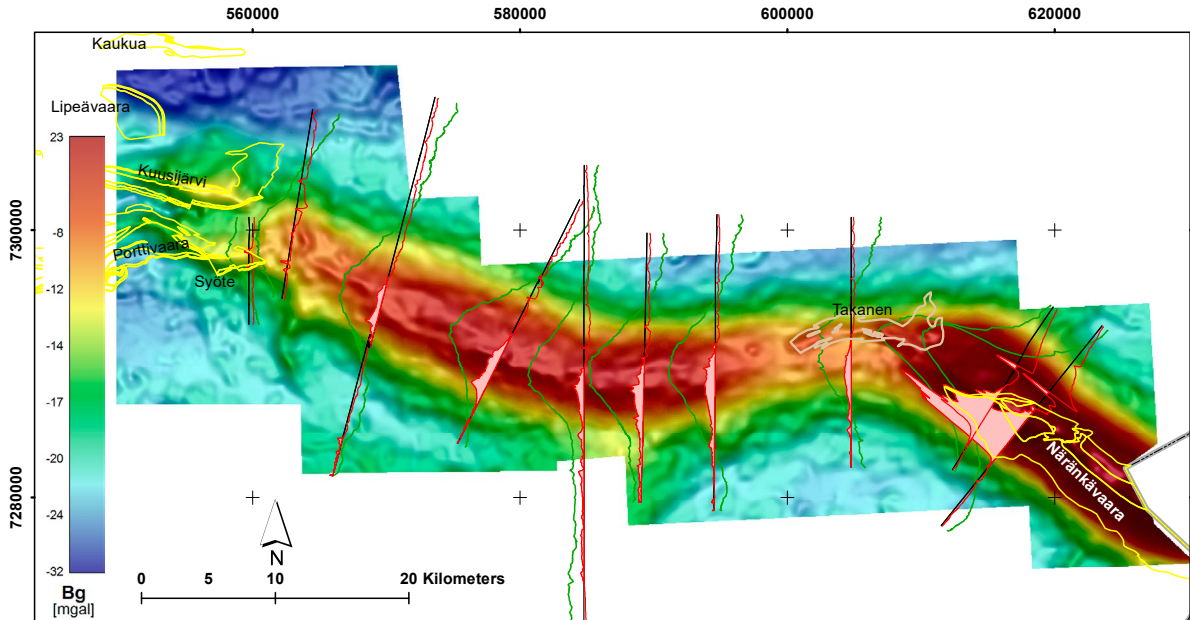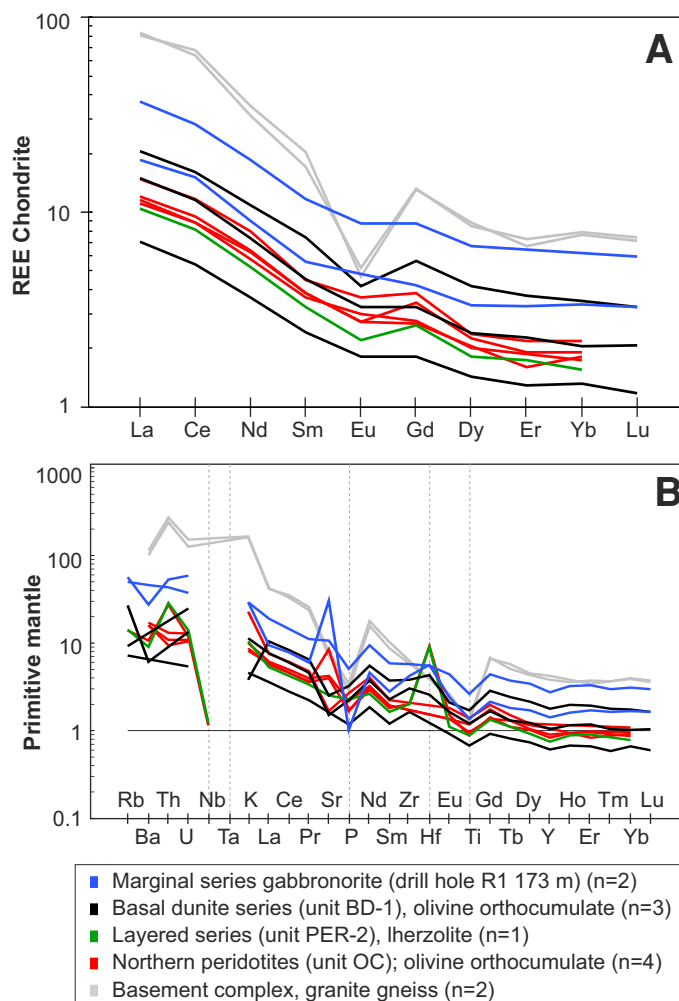
Figure 6. Modeled Bouguer data of the large linear positive gravity and magnetic anomaly (called the "hidden dyke") connecting the Näränkävaara intrusion in the east to the Koillismaa intrusion blocks in the west (yellow outlines). Note overlapping Archean Takanen greenstone belt (labeled, grey outline). Profiles show total magnetic intensity (red) and gravity (green); note similar displacement of magnetic maximum to south of the gravity maximum both over the Näränkävaara intrusion and elsewhere along the anomaly. Map by H. Salmirinne.

but the environments of formation invoked are very different. In komatiites, adcumulus formation is attributed to fast turbulent flow of lava supplying chemical components and flushing residual melt downstream (Hill et al. 1995; Arndt et al. 2008; Gole & Barnes 2020), whereas in intrusions adcumulate formation has been commonly attributed to near-equilibrium crystallization in the convecting and slow-cooling central parts of intrusions (Morse 1986; Campbell 1987; Walker et al. 1988; Latypov et al. 2020). Two different magma flow regimes in layered intrusions have been previously suggested by Latypov (2015), with examples (from the Koitelainen and Imandra intrusions) of initially fast-flowing magma forming accumulate marginal series, followed by orthocumulates formed in a more static convecting magma chamber (with less efficient stripping of solute). Recently, Lesher (2019) advocated channelized magma flow in mafic-ultramafic intrusive systems as an important mechanism for

accumulate formation. The abundant "extreme" olivine accumulates found in the basal dunite series can be interpreted as weakly differentiated cumulates formed in a channelized system (Lesher 2019). This interpretation is supported by the previously described sub-cotectic proportions of poikilitic chromite (Barnes 1998; Godel et al. 2013). It appears likely that magma influx fluctuated between continuous and discrete pulses during the formation of the basal dunite, with few periods of pooling, as evidenced by the aforementioned fluctuating Mg# values in olivine accumulates with height, and the fractionation of a single known orthopyroxenite layer (unit #5 in Fig. 2b) (Järvinen et al. 2021).

Magnetometric and gravimetric measurements show similarly offset peaks over both the Näränkävaara intrusion and the "hidden dyke" (Fig. 6). While this offset could be related to dip and its direction, we suggest that it could also result from differences in alteration and rock type observed

Figure 7. Whole-rock trace element compositions of key stratigraphic units (cf. Fig. 2) of the Näränkävaara intrusions in **a)** chondrite-normalized REE and **b)** primitive mantle-normalized trace element diagrams (Järvinen et al. 2020, 2021). Normalization values from Nakamura (1974) and McDonough & Sun (1995), respectively.

Marginal series gabbronorite (drill hole R1 173 m) (n=2)
Basal dunite series (unit BD-1), olivine orthocumulate (n=3)
Layered series (unit PER-2), lherzolite (n=1)
Northern peridotites (unit OC); olivine orthocumulate (n=4)
Basement complex, granite gneiss (n=2)

along the short axis of the Näränkävaara intrusion (e.g. *A* in Fig. 2c) (Järvinen et al. 2020, 2021). The olivine adcumulates of the basal dunite series are strongly serpentinized and of relatively low density, with formation of secondary magnetite making them highly magnetic. In contrast, the layered series pyroxenites to the north are almost unaltered and of relatively high density, with low abundances of magnetite making them weakly magnetic (note that the magnetic maximum along the northern border of the Näränkävaara intrusion in Fig. 6 is related to the northern peridotites; see Järvinen et al. 2022). In this case, Näränkävaara could represent an exposed part of the "hidden dyke" anomaly.

5.3. Emplacement of the Näränkävaara intrusion

Results of this and previous studies (Alapieti 1982; Järvinen et al. 2020, 2021) give evidence of multiphase emplacement history of the Näränkävaara intrusion from SHMB magmas. Parental magma compositions for the intrusion have been inferred from four independent units or sources (marginal series; zone BD-1 and unit PER-2; and weighted average of cross section *A* in Fig. 2a) (Järvinen et al. 2020, 2021, 2022). All show similar LREE-enriched SHMB parental magma compositions (Fig. 7), albeit with slightly decreasing Mg# upwards in stratigraphy (Table 1).

Slight variations in magma compositions can be attributed to magma fractionation in staging chambers. Isotope systematics in other 2.44 Ga Fennoscandian intrusions point to large-scale assimilation of Archean crust by mantle-plume sourced magmas rather than the magmas directly originating from an enriched sub-lithospheric mantle source (Amelin et al. 1995; Puchtel et al. 1997; Hanski et al. 2001a; Yang et al. 2016; Huhma et al. 2018). We interpret the origin of the Näränkävaara parental magmas to be the same, based on their inferred LREE-enrichment and negative initial ε_{Nd} values (Fig. 5). The fact that the initial, most primitive basal dunite magmas were already similarly LREE-enriched with generally similar negative initial ε_{Nd} values compared to later magma pulses (Fig. 5) suggests that the bulk of wall rock assimilation and homogenization had occurred by the initiation of the KLIC magmatism. Basement xenoliths and veins of felsic partial melts are commonly found in the marginal olivine orthocumulate units (Järvinen et al. 2021, 2022). These units show negligible intra-unit variation in initial ε_{Nd} values (Table 3) and generally homogeneous trace element composition, suggesting in situ contamination was not a significant process.

We suggest that the basal dunite series of the Näränkävaara intrusion formed from relatively primitive magmas in a dynamic magma feeder channel environment related to the KLIC magmatism. This was followed by formation of the layered series from slightly more evolved magmas in a more static and closed magma chamber environment after a decrease in magma influx. Magma influx began in the basal dunite series with initial primitive magmas forming orthocumulates along the present south-side of the intrusion, soon followed by pooling and fractionation forming the only known orthopyroxenite interlayer in the basal dunite (Figs. 8a, b) (Järvinen et al. 2021). These were followed by more voluminous and reduced magmas forming the ~1 km thick homogeneous olivine adcumulates with poikilitic chromite (Fig. 8c); again followed by pooling and formation

of olivine-orthopyroxene heteradcumulates at the top of the basal dunite series. During emplacement of the layered series magma, a non-cumulus textured and reversely fractionated marginal series gabbronorite was formed presently located between the layered series and basal dunite series with a tectonic contact to the latter (Fig. 8d). The position of the marginal series indicates either a magmatic hiatus between the formation of the basal dunite and the layered series (allowing for the required cooling of the basal dunite for the marginal series to form) or that the marginal series was originally formed against the granite-gneiss basement and later faulted to its current position (Järvinen et al. 2020). Nevertheless, after its initial emplacement the layered series seems to have crystallized in a relatively static setting (Fig. 8e), except for the two reversals caused by new magma pulses (PER-2 and PER-3 in Fig. 2b). These late recharge magmas were intruded along the northern side of the present intrusion, likely coinciding with faulting, where they formed orthocumulates (the northern peridotites) against the relatively cool basement gneiss (Figs. 8f–h) (Järvinen et al. 2022).

Based on our results, Näränkävaara represents the eastern part of an up to 100 km long intrusion complex composed of several pulses of mantle-derived fertile (variably metal depleted) magmas. LREE-enriched 2.44 Ga komatiites with similar trace-element and Nd-isotope composition are found in the Vetreny belt in Russian Karelia (Fig. 1) (Puchtel et al. 1997). Mafic-ultramafic volcanic rocks of this age group have not been dated in Finland, but 2.44 Ga felsic volcanic rocks are found near the Akanvaara layered intrusion in the Central Lapland Greenstone Belt (sample A1524 in Huhma et al. 2018). It can be speculated that Näränkävaara acted as a feeder for high-Cr and high-MgO basalts, similar to those described from the roughly contemporaneous Kuusamo group (Hanski & Huhma 2005; Köykkä et al. 2022). Transport of Näränkävaara-type fertile magma into smaller-scale subvolcanic feeder channels (e.g., sill-dyke networks or chonoliths; Magee et al. 2016) within volcanosedimentary supracrustal belts could
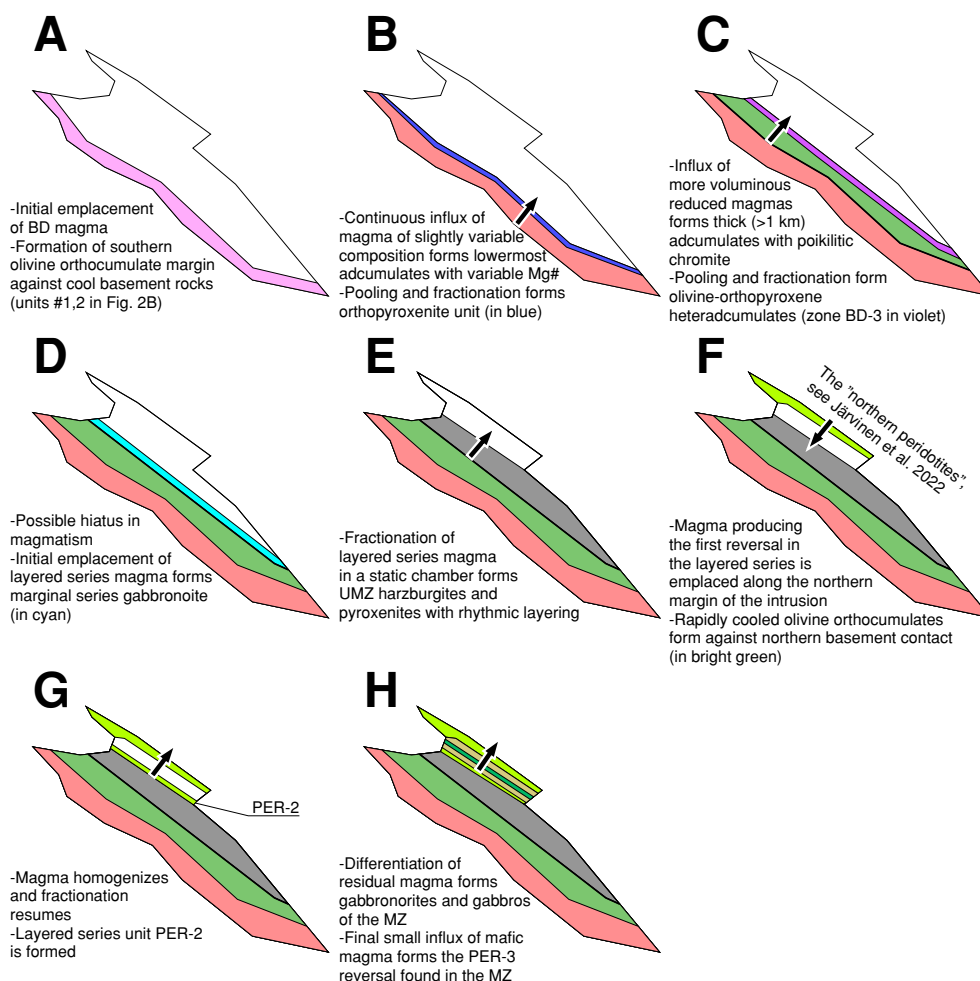
Figure 8. Schematic model for the emplacement history of the Näränkävaara intrusion (Alapieti et al. 1979; Alapieti 1982; Järvinen et al. 2020, 2021, 2022). Arrow shows approximate top direction of crystallizing cumulates. **a)** Initial emplacement of basal dunite series, formation of southern olivine orthocumulate margin; **b)** high influx of (contaminated?) magma forms lowermost olivine adcumulates with back-and-forth variation in Mg#, followed by pooling of magma and formation of an orthopyroxenite layer (blue); **c)** magma influx resumes with more reduced (uncontaminated?) magmas, formation of ~1 km-thick homogeneous olivine adcumulates with poikilitic chromite and textures suggesting bimodal olivine grain size distributions; followed by further pooling, fractionation, and formation of olivine-orthopyroxene heteradcumulates (violet, unit BD-3 in Fig. 2b); **d)** possible hiatus in magmatism, emplacement of layered series magma and formation of marginal series gabbronorite (cyan); **e)** static fractionation and formation of UMZ; **f)** emplacement of magma causing PER-2 reversal, formation of northern orthocumulate margin (the "northern peridotites"; see Järvinen et al. 2022); **g)** chamber homogenizes, unit PER-2 (and uneconomic SL reef) and base of MZ form; **h)** static fractionation of residual magma in chamber, influx of small batch of primitive magma forms unit PER-3 (turquoise), formation of MZ resumes and continues up to quartz diorites.

represent potential Ni-Cu-PGE exploration targets (Barnes et al. 2016; Lesher 2019).

The small Archean 2.95 Ga Takanen greenstone belt is found along the geophysical "hidden dyke" structure (Fig. 2a) (Karampelas 2022). Takanen is composed of komatiitic and bimodal volcanosedimentary rocks, and has been interpreted autochthonous. The "hidden dyke" may thus represent a long-lived trans-lithospheric structure (Begg et al. 2010), which acted as a pathway for mantle-sourced magmas in both the Archean (Takanen) and Paleoproterozoic (KLIC) (Tiira et

al. 2014; Gorczyk et al. 2018). The Takanen belt contains several S-rich volcanosedimentary layers (Iljina 2003; Karampelas 2022) and represents a possible source of external sulfur for the fertile 2.44 Ga magmas. This system has high potential for orthomagmatic Ni-Cu-PGE deposits (Barnes et al. 2016; Begg et al. 2018; Lesher 2019; Bleeker & Kamo 2020), but no evidence of 2.44 Ga igneous rocks in Takanen has been found (Karampelas 2022).

6. Conclusions

Our main conclusions are the following:

- Based on the presented U-Pb ID-TIMS baddeleyite ages, the basal dunite series was emplaced at 2441.7 ± 0.9 Ma, and is thus contemporaneous with the 2436 ± 5 Ma layered series. The most primitive parental magma composition has been inferred from the basal dunite series and the new baddeleyite age most likely marks the beginning of the Näränkävaara magmatism.

- Similarities in U-Pb ages, Sm-Nd isotope compositions, and independently inferred parental magma compositions indicate that the Näränkävaara basal dunite series and the layered series have formed from repeated emplacement of relatively homogeneous LREE-enriched SHMB magmas. Initial ε_{Nd} values around -2 are similar to those from other 2.44 Ga intrusions in northern Finland and Fennoscandia, and suggest parental magmas were derived from a mantle-plume source and subsequently contaminated with crustal materials. Homogeneity of parental magmas suggests contamination had mostly occurred in-bulk before emplacement.

- The Näränkävaara intrusion has formed from several pulses of Ni- and Cr-rich high-MgO basaltic magma. The basal dunite marks the beginning of this magmatism with a more primitive composition (Fo_{90-91}, 700 ppm Ni, and ε_{Nd} -1.8), whereas the layered series formed from more fractionated magmas with olivine ranging between Fo_{87-82} and initial ε_{Nd} between -2 to -2.4. In the beginning, magma was fed into the Näränkävaara chamber (or channel) on the southern side of the present intrusion, but magma flow had moved to the northern side by the emplacement of the PER-2 magma.

- The basal dunite exhibits several lithologic features that are commonly described from open-system komatiitic cumulate flows, suggesting (at least in part) origin as a magmatic feeder channel cumulate. No direct links to extrusive rocks in adjacent supracrustal belts are found, but the age, Sm-Nd isotope compositions and major and trace element compositions of the basal dunite series are very similar to the Vetreny belt komatiites and komatiitic basalts.

- Channelized mafic intrusions, as suggested for the basal dunite series of the Näränkävaara intrusion, are prospective for magmatic Ni-Cu-PGE sulfide deposits. The Takanen greenstone belt, hosting volcanogenic sulfides, overlaps with the 100 km-long KLIC system, and may have provided an external sulfur source for potential 2.44 Ga magmas.

- There may be a short hiatus in magmatism between the Näränkävaara basal dunite series and layered series, as evidenced by the marginal series found between the two series. However, the current location of the marginal series may also be explained by post-magmatic faulting.

Acknowledgements

References

Akkerman, J. H., 2008. Koillismaa-Naranka project (2005–2007). Geological Survey of Finland, Exploration report, 42 pp.

Alapieti, T.,1982. The Koillismaa layered igneous complex, Finland – its structure, mineralogy and geochemistry, with emphasis on the distribution of chromium. Geological Survey of Finland, Bulletin 319, 116 p.

Alapieti, T., Hugg, R., Piirainen, T. & Ruotsalainen A., 1979. The ultramafic and mafic intrusion at Näränkävaara, northeastern Finland. Geological Survey of Finland, Report of Investigation 35, 31 p.

Alapieti, T. T., Filén, B. A., Lahtinen, J. J., Lavrov, M. M., Smolkin & V. F., Voitsekhovsky, S. N., 1990. Early Proterozoic Layered Intrusions in the Northeastern Part of the Fennoscandian Shield. Mineralogy and Petrology 42, 1–22. https://doi.org/10.1007/BF01162681

Amelin, Y. V., Heaman, L. M. & Semenov, V. S., 1995. U-Pb geochronology of layered mafic intrusions in the Eastern Baltic Shield: implications for the timing and duration of Paleoproterozoic continental rifting. Precambrian Research 75, 31–46.
https://doi.org/10.1016/0301-9268(95)00015-W

Amelin Y. V. & Semenov V. S., 1996. Nd and Sr isotopic geochemistry of mafic layered intrusions in the eastern Baltic shield: implications for the evolution of Paleoproterozoic continental mafic magmas. Contributions to Mineralogy and Petrology 124:255–272. https://doi.org/10.1007/s004100050190

Arndt, N., Lesher, C. M. & Barnes, S. J., 2008. Komatiite. Cambridge University Press, Cambridge. 467 p.
https://doi.org/10.1017/CBO9780511535550

Barnes, S. J., 1998. Chromite in komatiites, 1. Magmatic controls on crystallization and composition. Journal of Petrology 39, 1689–1720.
https://doi.org/10.1093/petroj/39.10.1689

Barnes, S. J., Cruden, A. R., Arndt, N., Saumur, B. M., 2016. The mineral system approach applied to magmatic Ni-Cu-PGE sulphide deposits. Ore Geology Reviews 76, 296–316.
https://doi.org/10.1016/j.oregeorev.2015.06.012

Bayanova, T.B., 2006. Baddeleyite: A Promising Geochronometer for Alkaline and Basaltic Magmatism. Petrology 14, 187–200.
https://doi.org/10.1134/S0869591106020032

Bayanova T., Korchagin A., Mitrofanov, A., Serov, P., Ekimova, N., Nitikina, E., Kamensky, I., Elizarov, D. & Huber, M., 2019. Long-Lived Mantle Plume and Polyphase Evolution of Palaeoproterozoic PGE Intrusions in the Fennoscandian Shield. Minerals 9, 22 p.
https://doi.org/10.3390/min9010059

Begg, G. C., Hronsky, J. A. M., Arndt, N. T., Griffin, W. L., O'Reilly, S. Y. & Hayward, N., 2010. Lithospheric, Cratonic, and Geodynamic Setting of Ni-Cu-PGE Sulfide Deposits. Economic Geology 105, 1057–1070.
https://doi.org/10.2113/econgeo.105.6.1057

Begg, G. C., Hronsky, J. M., Griffin, W.L. & O'Reilly, S. Y., 2018. Global- to deposit-scale controls on orthomagmatic Ni-Cu-(PGE) and PGE reef ore formation. In: Mondal, S. K. & Griffin, W. L. (eds.), Processes and Ore Deposits of Ultramafic-Mafic Magmas through Space and Time. Elsevier, pp. 1–46.
https://doi.org/10.1016/B978-0-12-811159-8.00002-0

Bleeker, W. & Kamo, S., 2020. Structural-stratigraphic setting and U-Pb geochronology of Ni-Cu-Co-PGE ore environments in the central Cape Smith Belt, Circum-Superior Belt. In: Bleeker, W. & Houlé, M. G. (eds.), Targeted Geoscience Initiative 5: Advances in the understanding of Canadian Ni-Cu-PGE and Cr ore systems – Examples from the Midcontinent Rift, the Circum-Superior Belt, the Archean Superior Province, and Cordilleran Alaskan-type intrusions. Geological Survey of Canada, Open File 8722, pp. 65–98.
https://doi.org/10.4095/326882

Bohrson, W. A., Spera, F. J., Heinonen, J. S., Brown, G. A., Scruggs, M. A., Adams, J. V., Takach, M. K., Zeff, G., Suikkanen, E., 2020. Diagnosing open-system magmatic processes using the Magma Chamber Simulator (MCS): part I—major elements and phase equilibria. Contributions to Mineralogy and Petrology 175, 29 p.
https://doi.org/10.1007/s00410-020-01722-z

Campbell, I. H., 1987. Distribution of orthocumulate textures in the Jimberlana intrusion. Journal of Geology 95, 35–53. https://doi.org/10.1086/629105

Chistyakov, A. & Sharkov, E. V., 2008. Petrology of the Early Paleoproterozoic Burakovsky Complex, Southern Karelia. Petrology 16, 63–86.
https://doi.org/10.1134/S0869591108010049

Duke, J. M., 1986. Petrology and economic geology of the Dumont Sill: an Archean intrusion of komatiitic affinity in northwestern Quebec. Geological Survey of Canada, Economic Geology Report 35, 56 p.
https://doi.org/10.4095/120607

Elo, S., 1992. Geophysical indication of deep fractures in the Näränkävaara-Syöte and Kandalaksha-Puolanka zones. In: Silvennoinen, A. (ed.), Deep fractures in the Paanajärvi-Kuusamo-Kuolajärvi area. Geological Survey of Finland, Special Paper 13, 43–50.

Gerstenberger, H. & Haase, G., 1997. A highly effective emitter substance for mass spectrometric Pb isotope ratio determinations, Chemical Geology 136, 309–312.

Godel, B., Barnes, S. J. Gürer, D., Austin, P. & Fiorentini, M. L., 2013. Chromite in komatiites: 3D morphologies with implications for crystallization mechanisms. Contributions to Mineralogy and Petrology 165, 173–189. https://doi.org/10.1007/s00410-012-0804-y

Gole, M. J. & Barnes, S. J., 2020. The association between Ni-Cu-PGE sulfide and Ni-Co lateritic ores and volcanic facies within the komatiites of the 2.7 Ga East Yilgarn Craton large igneous province, Western Australia. Ore Geology Reviews 116, 1–21. https://doi.org/10.1016/j.oregeorev.2019.103231

Gorczyk, W., Molde, D. R., Barnes, S. J., 2018. Plume-lithosphere interaction at craton margins throughout Earth history. Tectonophysics 746, 678–694. https://doi.org/10.1016/j.tecto.2017.04.002

Gualda, G. A. R., Ghiorso, M. S., Lemons, R. V. & Carley, T. L., 2012. Rhyolite-MELTS: A modified calibration of MELTS optimized for silica-rich, fluid-bearing magmatic systems. Journal of Petrology 53, 875–890. https://doi.org/10.1093/petrology/egr080

Halkoaho, T., 1993. The Sompujärvi and Ala-Penikka PGE reefs in the Penikat layered intrusion, Northern Finland. Ph. D. thesis, Acta Universitatis Ouluensis A249, University of Oulu, Finland, 122 pp.

Halkoaho, T. & Niskanen, M., 2011. Tutkimustyöselostus Paltamon kunnassa varhaisproterotsooisella Junttilanniemen kerrosintruusiolla Varisniemen ja Karhusaaren välisellä alueella suoritetuista Ni-Cu-PGE-malmitutkimuksista vuosina 2007–2010. Geological Survey of Finland, Exploration report, Hakku-database, 18 p.

Hanski, E. & Huhma, H., 2005. Central Lapland greenstone belt. In: Lehtinen, M. et al. (Eds.), Precambrian Geology of Finland – Key to the Evolution of the Fennoscandian Shield. Developments in Precambrian Geology 14. Elsevier, pp. 139–194.

Hanski, E., Walker, R. J., Huhma, H. & Suominen, I., 2001a. The Os and Nd isotopic systematics of c. 2.44 Ga Akanvaara and Koitelainen mafic layered intrusions in northern Finland. Precambrian Research 109, 73–102. https://doi.org/10.1016/S0301-9268(01)00142-5

Hanski, E., Huhma, H., Rastas, P. & Kamenetsky, V. S, 2001b. The Palaeoproterozoic Komatiite-Picrite Association of Finnish Lapland. Journal of Petrology 42, 855–876. https://doi.org/10.1093/petrology/42.5.855

Hill, R. E. T., Barnes, S. J. , Gole, M. J. & Downling, S. E., 1995. The volcanology of komatiites as deduced from field relationships in the Norseman-Wiluna greenstone belt, Western Australia. Lithos 34, 159–188. https://doi.org/10.1016/0024-4937(95)90019-5

Hoatson, D. M. & Keays, R. R., 1989. Formation of platiniferous sulfide horizons by crystal fractionation and magma mixing in the Munni Munni layered intrusion, west Pilbara Block, Western Australia. Economic Geology 84, 1775–1804. https://doi.org/10.2113/gsecongeo.84.7.1775

Hölttä, P., Heilimo, E., Huhma, H., Kontinen, A., Mertanen, S., Mikkola, P., Paavola, J., Peltonen, P., Semprich, J., Slabunov, A. & Sorjonen-Ward, P., 2012. The Archaean of the Karelia Province in Finland. In: Hölttä, P. (ed.), The Archaean of the Karelia Province in Finland. Geological Survey of Finland, Special Paper 54, pp. 21–71.

Huhma, H., Cliff, R. A., Perttunen, V. & Sakko, M., 1990. Sm-Nd and Pb isotopic study of mafic rocks associated with early Proterozoic continental rifting: the Peräpohja schist belt in northern Finland. Contributions to Mineralogy and Petrology 104, 367–379.

Huhma, H., Hanski, E., Kontinen, A., Vuollo, J., Mänttäri, I. & Lahaye, Y., 2018. Sm–Nd and U–Pb isotope geochemistry of the Palaeoproterozoic mafic magmatism in eastern and northern Finland. Geological Survey of Finland, Bulletin 405, 150 p.

Iljina, M., 2003. Pohjois-Suomen kerrosintruusiot 1996–2002, Loppuraportti. Geological Survey of Finland, Report of project, 24 p.

Iljina, M. & Hanski, E., 2005. Layered mafic intrusions of the Tornio-Näränkävaara belt. In: Lehtinen, M. et al. (eds.), Precambrian geology of Finland – key to the evolution of the Fennoscandian Shield. Developments in Precambrian Geology 14. Elsevier, pp. 101–137.

Iljina, M., Maier, W. D. & Karinen, T., 2015. PGE-(Cu-Ni) Deposits of the Tornio-Näränkävaara Belt of Intrusions (Portimo, Penikat, and Koillismaa). In: Maier, W. D. et al. (eds.), Mineral Deposits of Finland. Elsevier, pp. 134–164.

Jaffey, A. H., Flynn, K. F., Glendenin, L. E., Bentley, W. C. & Essling, A. M., 1971. Precision Measurement of Half-Lives and Specific Activities of ^{235}U and ^{238}U, Physical Review C, 1889–1906. https://doi.org/10.1103/PhysRevC.4.1889

Järvinen, V. & Halkoaho, T., 2022. Formation of poikilitic chromite in the basal dunite series of the 2.44 Ga Näränkävaara layered intrusion. In: Groshev N. Yu. & Yang S. H. (eds.), The Fennoscandian School of Ore Genesis in Layered Intrusions, December 20th, 2021, Online Workshop 2, Extended abstracts, Oulu 2022, pp. 14–17. https://doi.org/10.31241/ARLIN.2021.000

Järvinen, V., Halkoaho, T., Konnunaho, J., Heinonen, J. S. & Rämö, O. T., 2020. Parental magma, magmatic stratigraphy, and reef-type PGE enrichment of the 2.44 Ga mafic-ultramafic Näränkävaara layered intrusion, northern Finland. Mineralium Deposita

55, 1535–1560. https://doi.org/10.1007/s00126-019-00934-z

Järvinen, V., Halkoaho, T., Konnunaho, J., Heinonen, J. S. & Rämö, O. T., 2021. The basal dunite of the Precambrian mafic-ultramafic Näränkävaara intrusion: Petrogenetic considerations and implications to exploration. Mineralogy and Petrology 115, 37–61. https://doi.org/10.1007/s00710-020-00725-9

Järvinen, V., Halkoaho, T., Konnunaho, J., Heinonen, J. S., Karinen, T. & Rämö, O. T., 2022. Petrogenesis of the Paleoproterozoic Näränkävaara layered intrusion, northern Finland, Part I: the northern peridotites and their relationships with the layered series and recharge events. Part I submitted simultaneously with the current manuscript to the GSF Bulletin.

Karampelas, N., 2022. Petrography, lithology, geochemistry and geochronology of the Takanen greenstone belt, eastern Finland. M. Sc. Thesis, University of Helsinki, 79 p.

Karinen, T., 2010. The Koillismaa intrusion, northeastern Finland – evidence for PGE reef forming processes in the layered series. Ph. D. thesis, Geological Survey of Finland, Bulletin 404, 176 p.

Karinen, T., Heinonen, S., Konnunaho, J., Salmirinne, H., Lahti, I. & Salo, A., 2021. Koillismaa Deep Hole – Solving the mystery of a geophysical anomaly. In: Kukkonen, I. et al. (eds.), Lithosphere 2021, eleventh symposium on structure, composition and evolution of the lithosphere, Programme and Extended Abstracts, pp. 55–58.

Konnunaho, J. & Lahti, I., 2008. Tutkimustyöselostus Pudasjärven kaupungissa ja Yli-Iin kunnassa sijaitsevasta Kärppäsuon gabrosta sekä valtausalueilla Vengasoja 1 ja Sarvensuo 1 (kaivosrekisterinumerot 7974/2 ja 7974/1) tehdyistä malmitutkimuksista vuosina 2002–2008. Geological Survey of Finland, Exploration report, Hakku-database, 24 p.

Köykkä J., Lahtinen, R. & Manninen, T., 2022. Tectonic evolution, volcanic features and geochemistry of the Paleoproterozoic Salla belt, northern Fennoscandia: From 2.52 to 2.40 Ga LIP stages to ca. 1.92–1.90 Ga collision. Precambrian Research 371, 20 p. https://doi.org/10.1016/j.precamres.2022.106597

Kulikov, V. S., Bychkova, Y. V., Kulikova, V. V. & Ernst, R., 2010. The Vetreny Poyas (Windy Belt) subprovince of southeastern Fennoscandia: An essential component of the ca. 2.5–2.4 Ga Sumian large igneous provinces. Precambrian Research 183, 589–601. https://doi.org/10.1016/j.precamres.2010.07.011

Krogh, T.E., 1973. A low-contamination method for hydrothermal decomposition of zircon and extraction of U and Pb for isotopic age determinations. Geochimica et Cosmochimica Acta 37, 485–494. https://doi.org/10.1016/0016-7037(73)90213-5

Latypov, R., 2015. Basal Reversals in Mafic Sills and Layered Intrusions. In: Charlier B. et al. (Eds.), Layered Intrusions. Springer, pp. 259–293. https://doi.org/10.1007/978-94-017-9652-1_6

Latypov, R. M., Chistyakova, S. Yu., Namur, O. & Barnes, S. J., 2020. Dynamics of evolving magma chambers: textural and chemical evolution of cumulates at the arrival of new liquidus phases. Earth-Science Reviews 210, 32 p. https://doi.org/10.1016/j.earscirev.2020.103388

Lesher, M., 2019. Up, Down, or Sideways: Emplacement of Magmatic Ni-Cu-(PGE) Sulfide Melts in Large Igneous Provinces. Canadian Journal of Earth Sciences 56, 756–773. https://doi.org/10.1139/cjes-2018-0177

Ludwig, K. R., 2003. User's Manual for Isoplot 3.00: A Geochronological Toolkit for Microsoft Excel. Berkeley Geochronology Center, Special Publication 4, 72 p.

Makkonen, H. V., Halkoaho, T., Konnunaho, J., Rasilainen, K., Kontinen, A. & Eilu, P., 2017. Ni-(Cu-PGE) deposits in Finland – geology and exploration potential. Ore Geology Reviews 90, 667–696. https://doi.org/10.1016/j.oregeorev.2017.06.008

Magee, C., Muirhead, J. D., Karvelas, A., Holford, S. P., Jackson, C. A. L., Bastow, I. D., Schonfield, N., Stevenson, C. T. E., McLean C., McCarthy, W., & Shtukert, O., 2016. Lateral magma flow in mafic sill complexes. Geosphere 12, 809–841. https://doi.org/10.1130/GES01256.1

Maier, W. D. & Groves, D. I., 2011. Temporal and spatial controls on the formation of magmatic PGE and Ni–Cu deposits. Mineralium Deposita 46, 841–857. https://doi.org/10.1007/s00126-011-0339-6

McDonough, W. F. & Sun, S.-s., 1995. The composition of the Earth. Chemical Geology 120, 223–253. https://doi.org/10.1016/0009-2541(94)00140-4

Morse, S.A., 1986. Convection in aid of adcumulus growth. Journal of Petrology 27, 1183–1214. https://doi.org/10.1093/petrology/27.5.1183

Murck, B. W. & Campbell, I. H., 1986. The effects of temperature, oxygen fugacity and melt composition on the behaviour of chromium in basic and ultrabasic melts. Geochimica et Cosmochimica Acta 50, 1871–1887. https://doi.org/10.1016/0016-7037(86)90245-0

Nakamura, N., 1974. Determination of REE, Ba, Fe, Mg, Na and K in carbonaceous and ordinary chondrites. Geochimica et Cosmochimica Acta 38, 757–775. https://doi.org/10.1016/0016-7037(74)90149-5

Puchtel, I. S., Haase, K. M., Hofmann, A. W., Chauvel, C., Kulikov, V. S., Garbe-Schönberg, C.-D. & Nemchin, A. A., 1997. Petrology and geochemistry of crustally contaminated komatiitic basalts from the Vetreny Belt, southeastern Baltic Shield: Evidence for an early Proterozoic mantle plume beneath rifted Archean continental lithosphere. Geochimica et Cosmochimica Acta 61, 1205–1222. https://doi.org/10.1016/S0016-7037(96)00410-3

Rämö, O. T., Karinen, T. & Halkoaho, T., 2017. Nd-Sr isotopic constraints for the source of the western part of Koillismaa-Näränkävaara Layered Igneous Complex. In: Hölttä P. et al. (eds), 3rd Finnish National Colloquium of geosciences, Abstract book. Geological Survey of Finland, Guide 63, pp. 77–78.

Sorjonen-Ward, P., Luukkonen, E. J., 2005. Archean Rocks. In: Lehtinen, M. et al. (Eds.), Precambrian Geology of Finland – Key to the Evolution of the Fennoscandian Shield. Developments in Precambrian Geology 14. Elsevier, pp. 19–99.

Steiger, R. H. & Jager, E., 1977. Subcommission on geochronology; Convention on the use of decay constants in geo- and cosmochronology. Earth and Planetary Science Letters 36, 359–362. https://doi.org/10.1016/0012-821X(77)90060-7

Telenvuo, B., 2017. Kumulusstratigrafia ja mineraalien kryptinen vaihtelu Kuusamon Näränkävaaran kerrosintruusion luoteisosassa. M. Sc. thesis, University of Oulu, 83 p.

Tiira, T., Janik, T., Kozlovskaya, E., Grad, M., Korja, A., Komminaho, K., Hegedus, E., Kovacs, C. A., Silvennoinen, H., Bruckl, E., 2014. Crustal Architecture of the Inverted Central Lapland Rift Along the HUKKA 2007 Profile. Pure and Applied Geophysics 171, 1129–1152. https://doi.org/10.1007/s00024-013-0725-3

Vaasjoki, M., 1977. Rapakivi granites and other postorogenic rocks in Finland: their age and elad isotopic composition of certain associated galena mineralizations. Geological Survey of Finland, Bulletin 294, 66 p.

Vesanto, J., 2003. Kaivoslain 19 §:n mukainen tutkimustyöelostus Kuusamon Näränkävaaran kerrosintruusion alueella valtauksilla Murtovaara 1–5, 7, 20, 30, 31, 36, 37, 41–71 suoritetuista malmitutkimuksista. Geological Survey of Finland, Exploration report, Hakku-database, 9 p.

Walker, D., Jurewicz, S. & Watson, E. B., 1988. Adcumulus dunite growth in a laboratory thermal gradient. Contributions to Mineralogy and Petrology 99, 306–319. https://doi.org/10.1007/BF00375364

Wilson, A. H., 1996. The Great Dyke of Zimbabwe. In: Cawthorn RG (ed.), Layered Intrusions, Developments in Petrology 15. Elsevier, pp. 365–402.

Yang, S., Hanski, E., Li, C., Maier, W. D., Huhma, H., Mokrushin, A. V., Latypov, R., Lahaye, Y., O'Brien, H. & Qu, W.-J., 2016. Mantle source of the 2.44–2.50-Ga mantle plume-related magmatism in the Fennoscandian Shield: evidence from Os, Nd, and Sr isotope compositions of the Monchepluton and Kemi intrusions. Mineralium Deposita 51, 1055–1073. https://doi.org/10.1007/s00126-016-0673-9